ANALYSIS OF FLOW OVER A WING WITH FEATHER LIKE WINGLETS

Jubear Shaik [1] , Dr. Viswanath Bellie[2]
[1]PG Scholar, M.Tech Aeronautical Engineering& N.H.C.E, Bengaluru,
[2]Professor of Dept of Mechanical Engineering, N.H.C.E, Bengaluru,

Abstract-- A numerical study was undertaken to study the effect of plain and feathers winglet configuration on the performance of a 3D wing at a velocity of 20 m/s and angle of attack of 6, 8 and 10^o. Baseline configurations along with four different winglet configurations were studied. The winglets studied are the blended type toward top and bottom and feathered winglets on the top and bottom side. A validation study was undertaken and it was found that the force values predicted by the software were very close to the forces measured in the experiments conducted over a 3D wing at higher angle of attack of 14^o .The chord wise pressure distribution was seen to change with the span wise location between the root and the tip and this distribution is affected by the wing tip vortex The wingtip was observed to change the pressure distribution near the tip The velocity field, stream lines and the vorticity were seen to be affected by the presence of the wing tip The lift and drag values were seen to increase with the angle of attack. Both the lift and drag values increase with the addition of the winglet compared to the baseline case. However, the increase in the area due to the addition of the winglet was considered to be the change in lift and drag. The ratio of lift to drag is seen to be affected with minor changes due to the addition of the winglets. The drag polar analysis revealed that the addition of winglet leads to get a higher lift for the same amount of drag. This is observed for all the winglet configurations. The winglet toward the top direction is seen to perform better than the winglet toward the bottom direction. Irrespective of the side where the winglets were added, feathered winglets performed better than the plain winglets breaking of the wingtip vortex. This may be the cause behind the better performance of the feathered winglets.

Keywords – plain and feathers winglet configuration, angle of attack, pressure distribution, drag polar analysis and lift to drag ratio.

I. INTRODUCTION

The need to reduce the impact of the aircraft emission on the environment is one of the active research areas in the aeronautical industry. One of the key mechanisms toward that is the reduction in drag. With the reduction in drag, the efficiency of the aircraft increases and it can fly to a higher range for the same amount of fuel and for the same fuel, increase in aircraft load such as passengers or freight can be increased. The amount of carbon that is emitted in the jet exit is also reduced which have a weaker impact on the environment. Wingtip induces a drag due to the vortex that is created by the flow between the bottom and the top surface. The difference in pressure between the bottom and top surface is the cause of the wing tip vortex. The schematic of the wingtip vortex is shown in figs 1.1 and 1.2.

The efficiency of the lifting surface is defined by the ratio between lift and the drag. This defines the ability of the object to produce lift beside the drag created by it. Higher L/D reveals that the object is able to produce higher lift for a given drag. So to get higher L/D ratios, two ways are possible. This is done by increasing the lift or by decreasing the drag. There are so many attempts reported in the literature to reduce the drag. Drag reduction is one of the active research areas among the aeronautical research field. Induced drag contributes by large fraction when the wing flies at higher angle of attack. This induced drag is proportional to the lift and inversely proportional to the aspect ratio.

The drag due to the wing tip vortex can be reduced by attaching surfaces near the wing tip. These surfaces are called winglets and their objective is to prevent the flow from the bottom surface to the top surface near the tip. There are different types of winglets are used and some of them are shown in fig 1.2.

As seen in fig 1.3, nature provides tiny feathers to the bird's wing. As discussed earlier, their function is to disturb the airflow around the tip. These feathers have advantages over conventional winglet as they can disturb the vortex development besides preventing the airflow around the tip. This tiny feathers neat the tip inspires the present work. In this work, it is proposed to study the effect of tiny feather like winglets on the characteristics of flow over a wing. The schematic of the proposed configuration is shown in fig 1.3. The variation in the winglet parameters (fig 1.3) will be studied to understand their effects on the flow field around the wing. A literature survey will be carried out and based on the literature survey, the operational parameters and sizing and the shape of the feather like winglet will be finalized.

Computational fluid dynamics will be used to carry out this work and the details are given below. The way the work will be carried out is shown in fig 1.3.

Characteristics or the development that will be studied

- Velocity, Pressure, Lift, drag and pitching moment

Fig 1.1: Effect of winglet on wingtip vortex

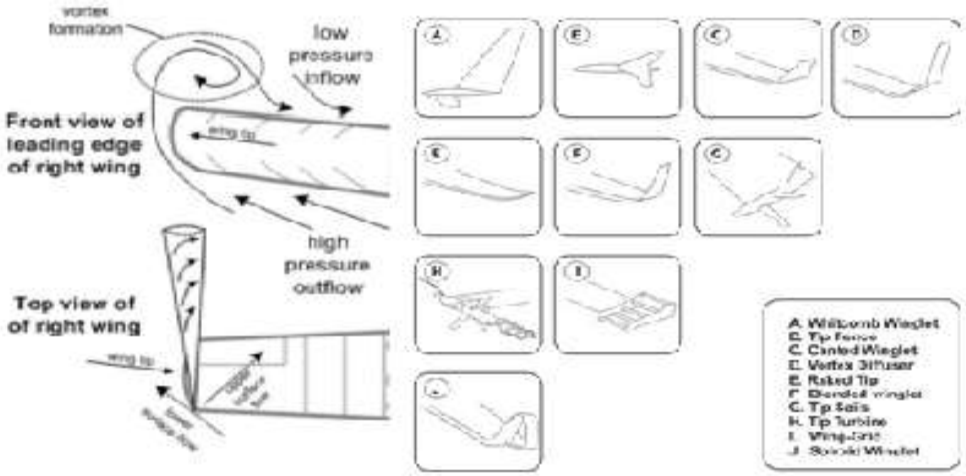

Fig 1.2: Concept of induced flow, Wingtip devices currently in use or in testing stage, from [1]

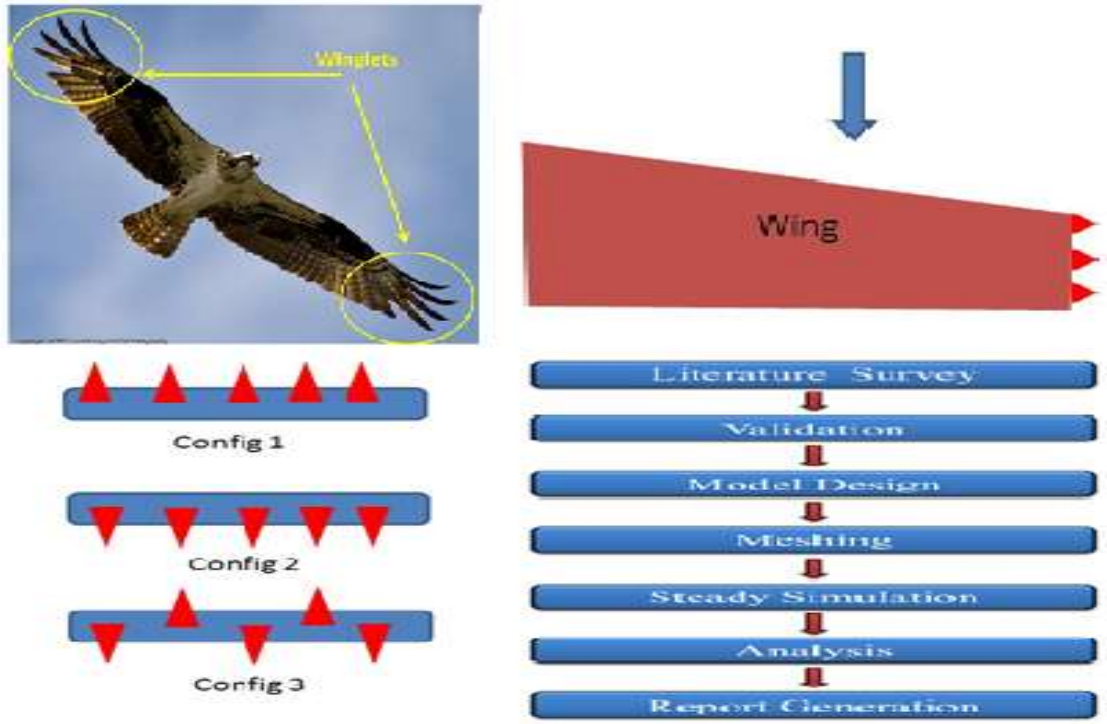

Fig 1.3: Tiny feathers acting like winglets in birds, Concept of wing with multi element winglet, Different winglet configurations (Side View), Methodology used in the present study

II. DESIGN OF THE MODEL

A) Baseline wing

The wing used in the baseline case is referred to the ONERA M6 wing. Schmitt and Charpin [7] studied the wing and published the data. They have given the dimensions of the wing. The dimensions given by them and photograph of the model used by them is given in figs 2.1 respectively.

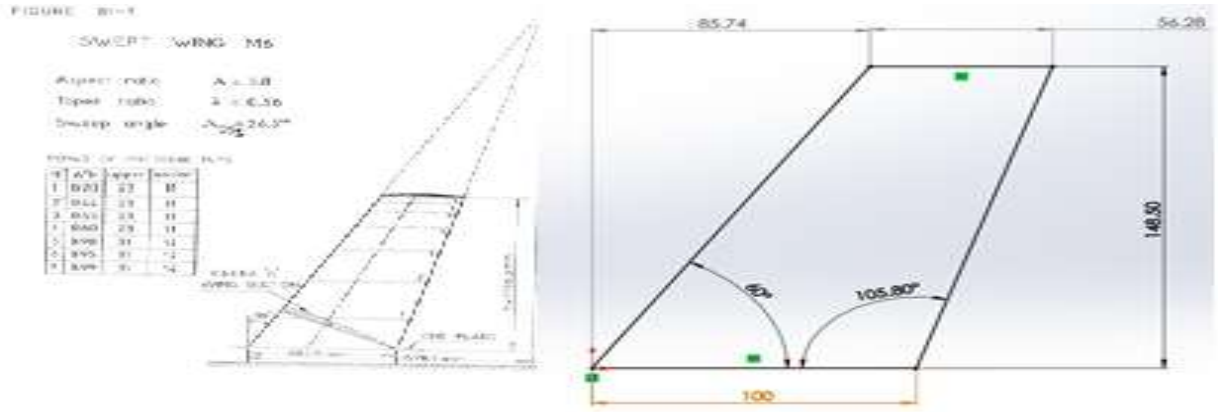

Fig 2.1: Dimensions of Onera wing model, Dimensions of the wing considered for the present study

The dimensions of the wing are referred and the wing is scaled down to have a root chord of 100 mm. The dimensions of the scaled down wing is shown in table 2.1.The winglet is designed based on the details given in the document by White comb [8] and Weierman [9]. The reference figs given in those documents are reproduced Based on these details, the winglet shape is determined and the basic shape of the winglet is shown in fig 2.2 the surface from the wingtip is extended along the shape given in this picture to obtain the basic winglet shape without the feather design. The wing with unfeathered winglet is shown in fig 2.2.

Fig 2.2: Details of the winglet shape, Baseline winglet towards the top and bottom

Fig 2.3: Feathered winglet on top, bottom view and both directions - 3D view

The feathers on the winglet are made by cutting the winglet. The size of the feathers and the gap between them is kept equal in the present study. This is done since no existing references are available on this spacing. Number of feathers is kept as 6. The 3D views of the wing with the feathers on the top side, winglet in bottom as well as both directions are shown in figs 2.3

III. GRID GENERATION

A) Variation of the models

The grids were generated mainly on five cases. They are

- Baseline wing - without winglet
- Wing with blended winglet toward top - without feathers
- Wing with blended winglet toward bottom - without feathers
- Wing with blended winglet toward top - with feathers
- Wing with blended winglet toward bottom - with feathers

These models have been discussed in the last. Out of these models, the models with winglet on both sides are not considered for further studies since, the tiny gaps in those models prevented meshing of the model. So those models were discarded.

B) Boundary condition

The boundary conditions are
Inlet velocity = 20 m/s is considered as velocity inlet
Inlet pressure (ambient pressure) = 101325 Pa
Outlet boundary condition was considered as a outflow
Sides are considered as wall boundary conditions.

To create the angle of attack, the flow should have components in horizontal and vertical direction. The velocity components in horizontal and vertical direction are calculated as given by eqns 3.1 and 3.2 respectively. This is justified by the fact that the aerofoil at an angle o attack for the horizontal flow is equal to the aerofoil at zero deg with the flow at the same angle.

$$V_x = V * cos(\theta) \quad (3.1)$$

$$V_y = V * sin(\theta) \quad (3.2)$$

The velocity components for different angles of attack of 6, 8 and 10 deg are calculated using the equations given above and they are given in the table 3.1.

TABLE *3.1:* COMPONENTS OF VELOCITY AT DIFFERENT α

Θ	V	V_x	V_y
6	20	19.89	2.09
8	20	19.8	2.783
10	20	19.696	3.473

C) Grid

The grid generated for the baseline case is shown in figs 3.1 the grid is made finer near the aerofoil surface and coarse far away from the aerofoil.

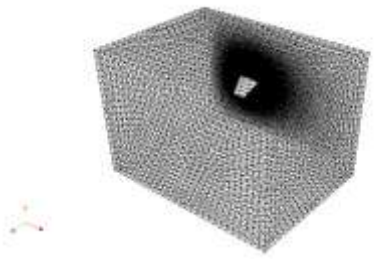

Fig 3.1: Grid generated for the baseline case

Grid for other models is also generated in similar manner and the grid generated for all the models is shown in figs 3.2.

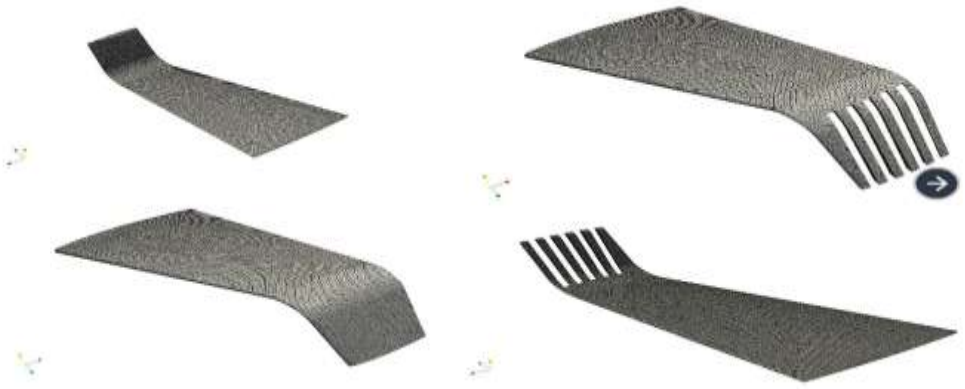

Fig 3.2: Grid generated for the winglet on top, bottom, bottom and top with feather

IV. RESULTS AND DISCUSSION

A) Pressure distribution

Pressure distribution on the top and bottom surface of the baseline aerofoil at 6 deg angle of attack is shown in fig 4.1.
As seen in the fig, the pressure reduces near the leading edge and gains its value in the downstream direction. The acceleration of the flow over the leading edge of the wing is the reason behind this. The pressure distribution looks almost uniform across the span wise direction. The pressure distribution on the bottom surface as shown in Fig 4.1 reveals the high pressure near the leading edge which is the stagnation region and the pressure distribution downstream of it looks uniform which is the typical pressure distribution over the bottom surface of the wing at 6 deg angle of attack.

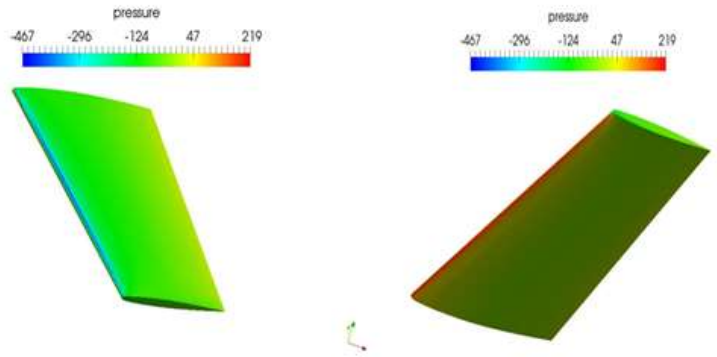

Fig 4.1: Pressure distribution on Top and bottom surface - Baseline at 6 deg

As seen in the fig, the pressure reduces near the leading edge and gains its value in the downstream direction. The acceleration of the flow over the leading edge of the wing is the reason behind this. The pressure distribution looks almost uniform across the span wise direction. The pressure distribution on the bottom surface as shown in Fig 4.1 reveals the high pressure near the leading edge which is the stagnation region and the pressure distribution downstream of it looks uniform which is the typical pressure distribution over the bottom surface of the wing at 6 deg angle of attack.

As seen in the fig, the pressure reduces near the leading edge and gains its value in the downstream direction. The acceleration of the flow over the leading edge of the wing is the reason behind this. The pressure distribution looks almost uniform across the span wise direction. The pressure distribution on the bottom surface as shown in Fig 4.1 reveals the high pressure near the leading edge which is the stagnation region and the pressure distribution downstream of it looks uniform which is the typical pressure distribution over the bottom surface of the wing at 6 deg angle of attack.

The pressure distribution over the top and bottom surface at 8 and 10 deg angle of attack for the baseline case is shown in figs 4.2. As seen in the figs, the pressure distribution on the top surface is different at high angle of attack of 10 deg. The pressure distribution near the tip is affected. This could be due to the wingtip vortex that is present at high angle of attack.
The effect of angle of attack at different span wise location on the top surface is shown in fig 4.3 and 4.4.

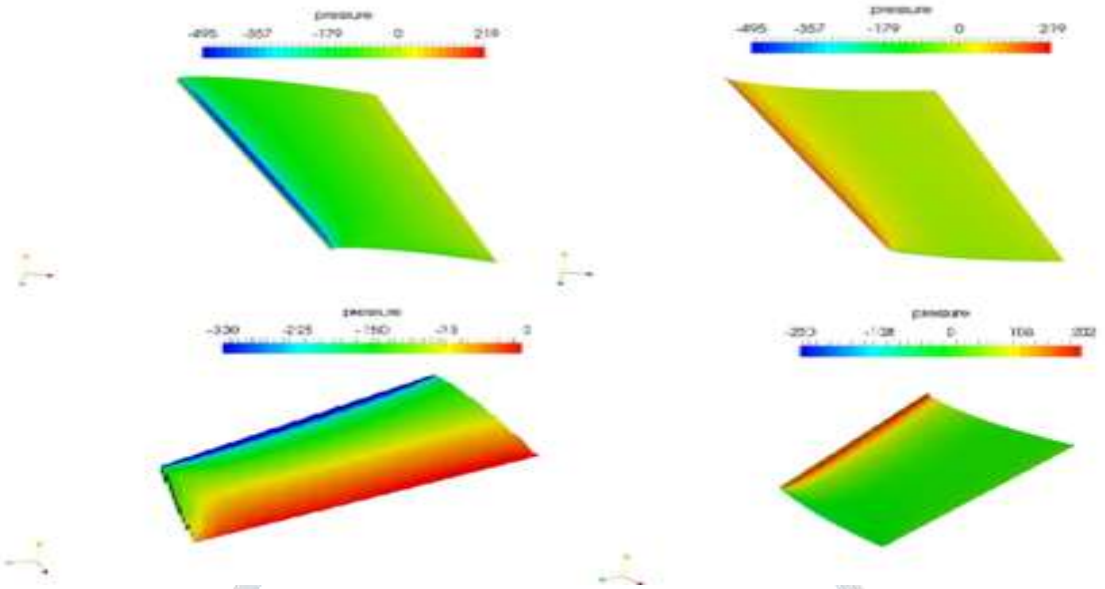

Fig 4.2: Pressure distribution on top and bottom surface - Baseline at 8 and 10 deg

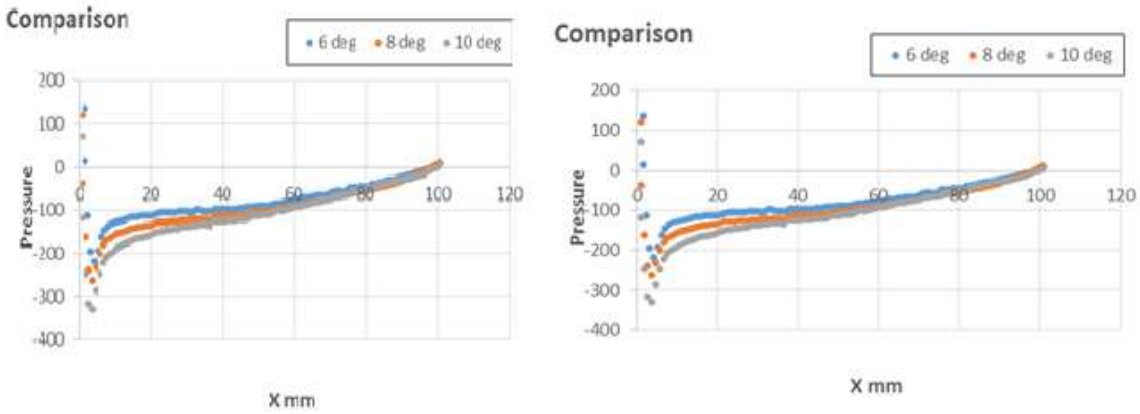

Fig 4.3: Comparison of pressure distribution on top surface - z = 0 mm

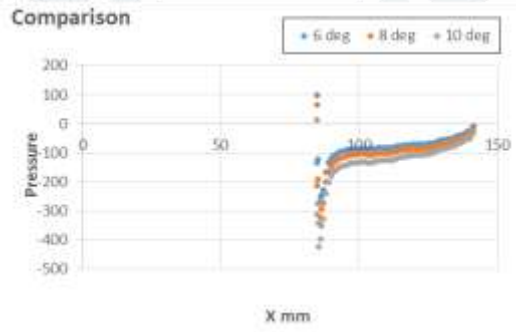

Fig 4.4: Comparison of pressure distribution on top surface - z = 145 mm

The pressure contour formed on top surface of wing with winglet toward top as shown in fig 4.5 shows that the pressure distribution is modified by the presence of the winglet. Similar kind of pressure distribution can be seen for the wing with the winglet toward bottom as shown in fig. 4.5.

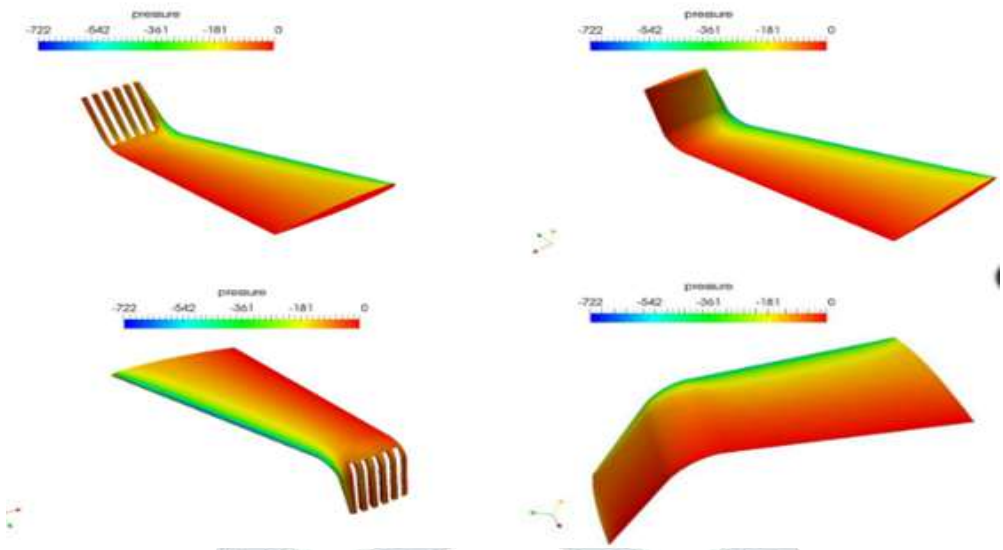

Fig 4.5: Pressure distribution on top surface of wing with winglet toward top at 10 deg, feather winglet toward bottom, feather winglet toward top - Zoomed View

The feather winglet also affects the pressure distribution on the top surface of the wing. The pressure distribution for the wing with the feather winglet on top side is shown in fig 4.5.

Though the area of the effective winglet is reduced, minor change in pressure distribution can be seen between the feathers of the winglet. This can be due to the airflow between the feathers. The pressure distribution for the wing with the feathered wing toward bottom is shown in fig 4.5. This pressure distribution also shows that minor change in pressure is observed near the feather surfaces.

B) Vorticity

The distribution of the vorticity at the plane normal to the x axis at 350 mm for different configurations at 10 deg angle of attack is shown in figs 4.6. The vorticity contours are plotted against the same contour level for ease of comparison. As seen in the fig 4.6 for baseline case, the vorticity is concentrating near the wing tip and the size of the wing tip vortex is also large compared to other configurations. When unfeathered winglets are used in top and bottom sides, the size of the vortex also reduces and the vorticity is seen to follow the shape of the winglet just downstream of it. Further to this, when feathered winglets are used, they are reducing the vorticity levels further than the unfeathered winglets, and the region of maximum vorticity also reduces in size. These pictures show the effect of different winglet configurations on the distribution of the vorticity just downstream of the wing.

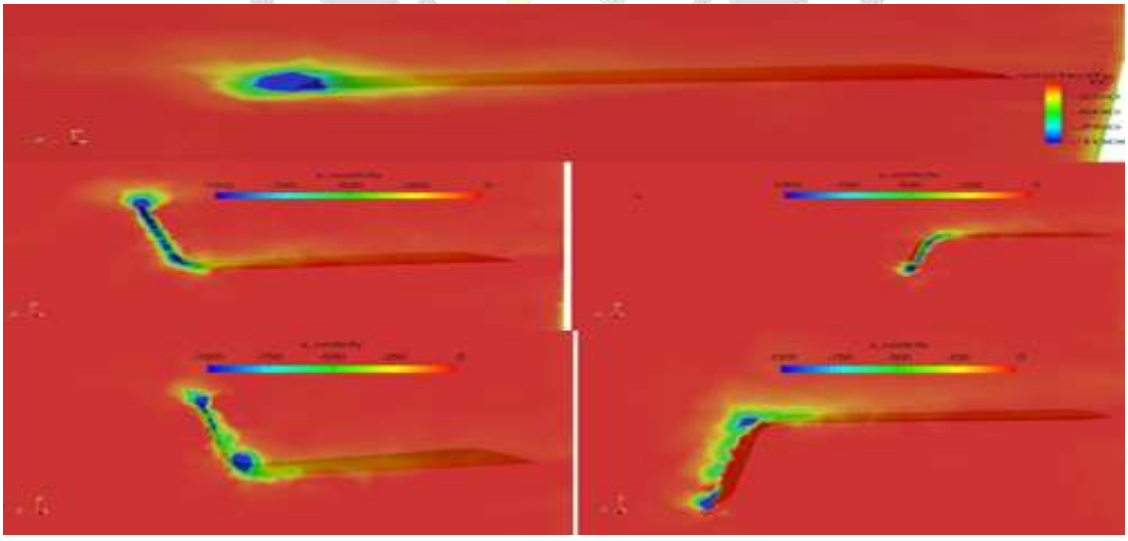

Fig 4.6: Vorticity at x=350 mm, Baseline at 10 deg, Winglet on top, Winglet on bottom, Feathered winglet on top, Feathered winglet on bottom.

The streamlines for different configurations are shown in figs 4.7. As seen in the figs, the baseline wing results in the flow going around the wing. However, this curly motion is avoided in the winglet on the top and bottom. When feathered winglets are used, they split the curling flow further and the stream lines are seen to enter between the gaps provided by the feathers. This can be the reason behind the effective disintegration of the wing tip vortex. The disintegration of the flow field can be clearly seen in figs 4.7. Where the stream lines show

the effectiveness of the feathered winglet configurations.

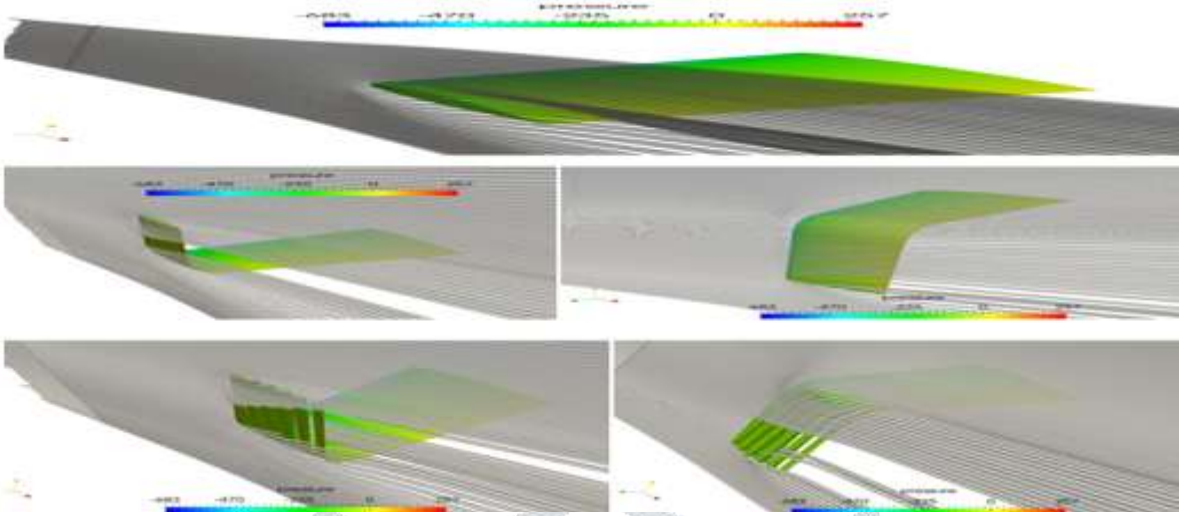

Fig 4.7: Streamlines – baseline, winglet on top, bottom, feathered winglet on top and bottom at 10 deg

C) Aerodynamic coefficients

This section discusses the aerodynamic coefficients on the wing at different angles of attack for various winglet configurations. The forces can be obtained in vertical and horizontal direction as seen in the fig. The walls of the wing alone are chosen to get the forces on the wing otherwise it would report the forces from other walls also.

The forces obtained through this in vertical and horizontal direction are the forces that are normal and the parallel to the wing since the wing is at zero deg and the wind is blowing at an angle to simulate the angle of attack as seen in fig 4.8. The forces that are normal and parallel to the wing obtained through this method are shown in fig 4.8. However, the lift and drag forces are normal and parallel to the free stream respectively as shown in fig 4.8. The forces in the body normals are to be resolved in the wind normals. The forces are resolved using the equations 4.1 and 4.2.

$$L = N * Cos(\alpha) - P * Sin(\alpha) \qquad (5.1)$$

$$D = N * Sin(\alpha) + P * Cos(\alpha) \qquad (5.2)$$

Here, L = Lift, D = Drag, N = Normal forces, P = Parallel forces

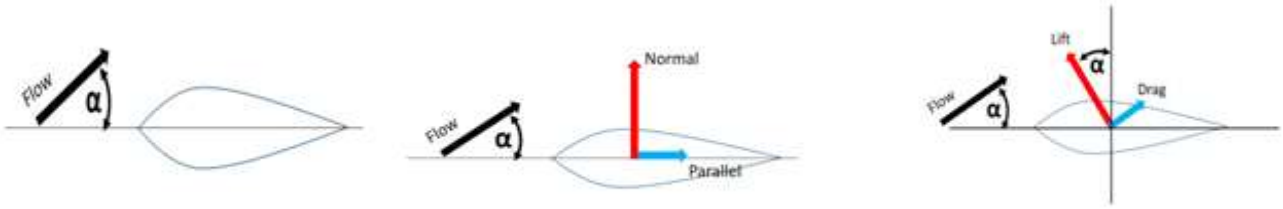

Fig 4.8: Schematic of setting up of the angle of attack in current study, Forces normal and parallel to the wing and to the free stream

The normal and parallel forces obtained from the software. The resolved forces that are normal and parallel to the free stream. The forces obtained through this method are non dimensionalised using the equations 4.3 and 4.4.

$$C_L = \frac{F_L}{0.5\rho v^2 A} \qquad (4.3)$$

$$C_d = \frac{F_d}{0.5\rho v^2 A} \qquad (4.4)$$

Where, $\rho = 1.225\ kg/m^3$

$v = 20\ m/s$

$S = A$ = *Reference area* = $11607\ mm^2$.

Here the lift is increasing with the addition of the winglets. This is valid for both the bottom and top winglets. However, it should be noted that the drag is also seen to increase. The addition of the surface are due to the winglet may be the reason for this. However, the ratio of lift to drag that defines the efficiency of the wing is not affected much except a few conditions.

The variation of coefficients is shown in fig 4.9. The increase in lift as well as the drag needs additional exploration. As Guerrero pointed

out in his paper [1], when winglets are added, the variation between CL and CD is to be looked at. He has done similar comparison as seen in fig 4.9. and he has pointed out that the capability to produce higher CL for the same CD can show the effectiveness of the winglet. Current results are also plotted in a similar manner and the same is shown in fig 4.9. As seen in the fig, with the addition of the winglet, the lift coefficient increases for a given coefficient of drag. However, addition of the winglet seems beneficial on the top over the addition of it to the bottom. Adding feather to the winglet increases this effect further where it is more effective on the top side than the bottom side. The foot print of the wing tip vortex that is left on the top side of the wing is more affected by the presence of the plain winglet and feathered winglet on the top side. This may be the reason behind the effective performance. Though the winglet on the bottom side is also effective, it is slightly inferior to the one on the top.

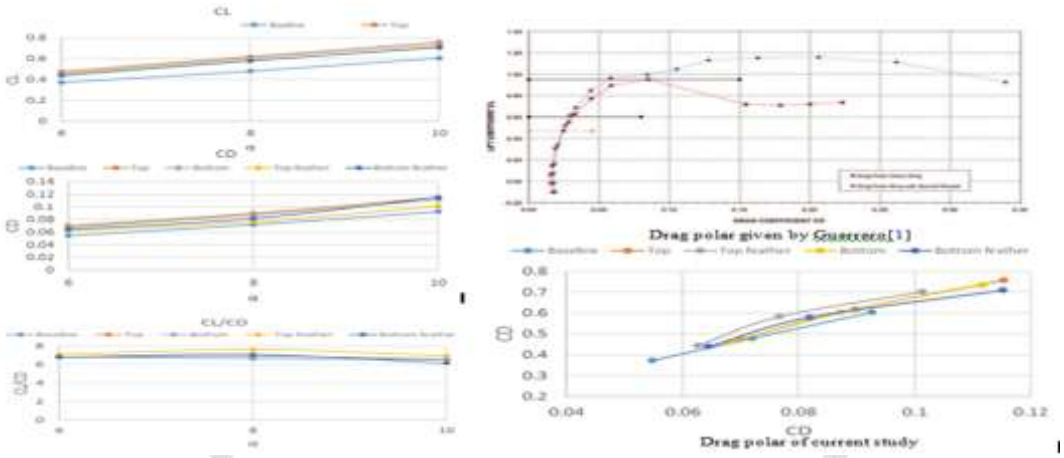

Fig 4.9: Variation of CL, CD, CL/CD, with different configuration, Drag polar given by Guerrero, Drag polar of current study

V.CONCLUSIONS

A numerical study was undertaken to study the effect of plain and feathers winglet configuration on the performance of a 3D wing at a velocity of 20 m/s and angle of attack of 6, 8 and 10^{o}.Baseline configurations along with four different winglet configurations were discussed. The winglets discussed are the blended type toward top and bottom and feathered winglets on the top and bottom side. A validation study was undertaken and it was found that the force values predicted by the software were very close to the forces measured in the experiments conducted over a 3D wing at higher angle of attack of 14 deg. The chord wise pressure distribution was seen to change with the span wise location between the root and the tip and this distribution is affected by the wing tip vortex. The wingtip was observed to change pressure distribution near the tip. The speed field, stream lines and vorticity are influenced by the existence of the wing tip. The lift and drag values were seen to increase with the angle of attack. Both the lift and drag values increase with the addition of the winglet compared to the baseline case. However, the increase in the area due to the addition of the winglet was considered to be the change in lift and drag. The ratio of lift to drag is seen to be affected with minor changes due to the addition of the winglets. The drag polar analysis revealed that the addition of winglet leads to get a higher lift for the same amount of drag. This is observed for all the winglet configurations. The winglet toward the top direction is seen to perform better than the winglet toward the bottom direction. Irrespective of the side where the winglets were added, feathered winglets performed better than the plain winglets. Breaking of the wingtip vortex which may be the cause behind the better performance of the feathered winglets

VI.FUTURE PLAN

For the present study, only 20 m/s is considered as the free stream velocity .This study needs to be extended to other free stream velocities. The effect of the wingtip configuration needs to be explored for the change in further α, winglet curvature and winglet dimensions.

ACKNOWLEDGEMENTS

I am grateful to Dr. M S Ganesha Prasad Dean & student's affairs and Hod of department of Mechanical Engineering, Mr. Chethan Kumar D. S, Senior Professor, department of Mechanical Engineering, for his unfailing encouragement and suggestion. I take this opportunity to express my profound gratitude to Principal, Dr.Manjunatha for his constant support and encouragement.

References

[1] J. E. Guerrero, D. Maestro, and A. Bottaro, "Biomimetic spiroid winglets for lift and drag control," *Comptes Rendus Mecanique*, vol. 340, no. 1, pp. 67–80, 2012.

[2] C. Thipyopas and N. Intaratep, "Aerodynamics study of fixed-wing mav: Wind tunnel and flight test," in *International Micro Air Vehicle conference and competitions 2011 (IMAV 2011),'t Harde, The Netherlands, September 12-15, 2011*, Delft University of Technology and Thales, 2011.

[3] S. R. Reddy, G. S. Dulikravich, A. Abdoli, and H. Sobieczky, "Multi-winglets: Multi-objective optimization of aerodynamic shapes," in *53rd AIAA Aerospace Sciences Meeting*, p. 1489, 2015.

[4] M. Smith, N. Komerath, R. Ames, O. Wong, and J. Pearson, "Performance analysis of a wing with multiple winglets," No. AIAA 2001-2407, 2001.

[5] S. C. Yen and Y. F. Fei, "Winglet dihedral effect on flow behavior and aerodynamic performance of naca0012 wings," *Journal of Fluids Engineering*, vol. 133, no. 7, p. 071302, 2011.

[6] G. Ananda, P. Sukumar, and M. Selig, "Measured aerodynamic characteristics of wings at low Reynolds numbers," *Aerospace Science and Technology*, vol. 42, pp. 392–406, 2015.

[7] V. Schmitt and F. Charpin, "Pressure distributions on the onera-m6-wing at transonic mach numbers," *Experimental data base for computer program assessment*, vol. 4, 1979.

[8] R. T. Whitcomb, "A design approach and selected wind tunnel results at high subsonic speeds for wing-tip mounted winglets," 1976.

[9] J. Weierman and J. Jacob, "Winglet design and optimization for uavs," in *28th AIAA Applied Aerodynamics Conference*, p. 4224, 2010.